Anal. Chem. **2009,** *81,* 9114–9119

Aptamer–DNAzyme Hairpins for Amplified Biosensing

Carsten Teller, Simcha Shimron, and Itamar Willner*

Institute of Chemistry, The Hebrew University of Jerusalem, Jerusalem, 91904 Israel

Engineered nucleic acid hairpin structures are used for the amplified analysis of low-molecular-weight substrates (adenosine monophosphate, AMP) or proteins (lysozyme). The hairpin structures consist of the anti-AMP or antilysozyme aptamer units linked to the horseradish peroxidase (HRP)-mimicking DNAzyme sequence. The HRP-mimicking DNAzyme sequence is protected in a "caged", inactive structure in the stem regions of the respective hairpins, whereas the loop regions include a part of the respective aptamer sequence. The opening of the hairpins by the analytes, AMP or lysozyme, through the formation of the respective analyte–aptamer complexes, results in the self-assembly of the active HRP-mimicking DNAzyme. The DNAzyme catalyzes the H_2O_2-mediated oxidation of 2,2′-azino-bis(3-ethylbenzothiazoline-6-sulfonic acid) ($ABTS^{2-}$) to the colored $ABTS^{\bullet-}$, thus providing the amplified optical detection of the respective analytes. The engineered aptamer–DNAzyme hairpin structures reveal significantly improved analytical performance, as compared to analogous fluorophore–quencher-labeled hairpins.

Aptamers are nucleic acids exhibiting specific recognition properties toward low-molecular-weight substrates or biopolymers. The aptamers are elicited by the systematic evolution of ligands by the exponential enrichment (SELEX) procedure.[1,2] Substantial recent research efforts are directed toward the development of electrochemical[3] or optical[4] aptasensors. Electrochemical aptasensors based on aptamers labeled with redox-active units,[5] redox proteins,[6] or electrocatalytic nanoparticles[7] were reported, and impedimetric aptamer-based sensors[8] or even label-free aptasensors[9] were designed on field-effect transistors. Various optical aptasensors that involve fluorophores,[10] quantum dots,[11] or metallic nanoparticles[12] were, similarly, developed. Also, catalytic nucleic acids (DNAzymes) find growing interest as catalytic labels to amplify biosensing events. For example, the horseradish peroxide-mimicking DNAzyme[13] was recently used as a catalytic label for the colorimetric or chemiluminescence detection of DNA or enzyme activities.[14] Furthermore, aptamer–DNAzyme conjugates[15] were used for analyzing aptamer–substrate complexes.

Numerous nucleic acid hairpin structures, particularly fluorophore–quencher hairpin beacons, were used to analyze DNA.[16–18] The hybridization of the analyte DNA to the single-stranded loop region of the structures results in the opening of the stem domain of the hairpins, leading to a change in the electrical or optical properties of the systems. Also, hairpin nucleic acid structures

* To whom correspondence should be addressed. E-mail: willnea@vms.huji.ac.il.

(1) (a) Ellington, A. D.; Szostak, J. W. *Nature* **1990**, *346*, 818–822. (b) Tuerk, C.; Gold, L. *Science* **1990**, *249*, 505–510.

(2) (a) Burgstaller, P.; Famulok, M. *Angew. Chem., Int. Ed.* **1994**, *33*, 1084–1087. (b) Lauhon, C. T.; Szostak, J. W. *J. Am. Chem. Soc.* **1995**, *117*, 1246–1257. (c) Geiger, A.; Burgstaller, P.; von der Eltz, H.; Roeder, A.; Famulok, M. *Nucleic Acids Res.* **1996**, *24*, 1029–1036. (d) Stojanovic, M. N.; de Prada, P.; Landry, D. W. *J. Am. Chem. Soc.* **2000**, *122*, 11547–11548. (e) Nitsche, A.; Kurth, A.; Dunkhorst, A.; Panke, O.; Sielaff, H.; Junge, W.; Muth, D.; Scheller, F.; Stocklein, W.; Dahmen, C.; Pauli, G.; Kage, A. *BMC Biotechnol.* **2007**, *7*, 48.

(3) Willner, I.; Zayats, M. *Angew. Chem., Int. Ed.* **2007**, *46*, 6408–6418.

(4) (a) Liu, J.; Cao, Z.; Lu, Y. *Chem. Rev.* **2009**, *109*, 1948–1998. (b) Gill, R.; Polsky, R.; Willner, I. *Small* **2006**, *2*, 1037–1041. (c) Pavlov, V.; Xiao, Y.; Shlyahovsky, B.; Willner, I. *J. Am. Chem. Soc.* **2004**, *126*, 11768–11769.

(5) (a) Xiao, Y.; Piorek, B. D.; Plaxco, K. W.; Heeger, A. J. *J. Am. Chem. Soc.* **2005**, *127*, 17990–17991. (b) Baker, B. R.; Lai, R. Y.; Wood, M. S.; Doctor, E. H.; Heeger, A. J.; Plaxco, K. W. *J. Am. Chem. Soc.* **2006**, *128*, 3138–3139. (c) Xiao, Y.; Rowe, A. A.; Plaxco, K. W. *J. Am. Chem. Soc.* **2007**, *129*, 262–263. (d) Freeman, R.; Li, Y.; Tel-Vered, R.; Sharon, E.; Elbaz, J.; Willner, I. *Analyst* **2009**, *134*, 653–656. (e) Zuo, X.; Xiao, Y.; Plaxco, K. W. *J. Am. Chem. Soc.* **2009**, *131*, 6944–6945.

(6) (a) Ikebukuro, K.; Kiyohara, C.; Sode, K. *Biosens. Bioelectron.* **2005**, *20*, 2168–2172. (b) Centi, S.; Messina, G.; Tombelli, S.; Palchetti, I.; Mascini, M. *Biosens. Bioelectron.* **2008**, *23*, 1602–1609.

(7) Polsky, R.; Gill, R.; Kaganovsky, L.; Willner, I. *Anal. Chem.* **2006**, *78*, 2268–2271.

(8) (a) Elbaz, J.; Shlyahovsky, B.; Li, D.; Willner, I. *ChemBioChem* **2008**, *9*, 232–239. (b) Sharon, E.; Freeman, R.; Tel-Vered, R.; Willner, I. *Electroanalysis* **2009**, *21*, 1291–1296.

(9) (a) So, H.; Won, K.; Kim, Y. H.; Kim, B.; Ryu, B. H.; Na, P. S.; Kim, H.; Lee, J. *J. Am. Chem. Soc.* **2005**, *127*, 11906–11907. (b) Zayats, M.; Huang, Y.; Gill, R.; an Ma, C.; Willner, I. *J. Am. Chem. Soc.* **2006**, *128*, 13666–13667.

(10) (a) Stojanovic, M. N.; de Prada, P.; Landry, D. W. *ChemBioChem* **2001**, *2*, 411–415. (b) Tang, Z.; Mallikaratchy, P.; Yang, R.; Kim, Y.; Zhu, Z.; Wang, H.; Tan, W. *J. Am. Chem. Soc.* **2008**, *130*, 11268–11269. (c) Rajendran, M.; Ellington, A. *Anal. Bioanal. Chem.* **2008**, *390*, 1067–1075.

(11) (a) Dwarakanath, S.; Bruno, J. G.; Shastry, A.; Phillips, T.; John, A.; Kumar, A.; Stephenson, L. D. *Biochem. Biophys. Res. Commun.* **2004**, *325*, 739–743. (b) Levy, M.; Cater, S. F.; Ellington, A. D. *ChemBioChem* **2005**, *6*, 2163–2166. (c) Hansen, J. A.; Wang, J.; Kawde, A.; Xiang, Y.; Gothelf, K. V.; Collins, G. *J. Am. Chem. Soc.* **2006**, *128*, 2228–2229.

(12) (a) Liu, J.; Lu, Y. *Angew. Chem., Int. Ed.* **2006**, *45*, 90–94. (b) Wei, H.; Li, B.; Li, J.; Wang, E.; Dong, S. *Chem. Commun.* **2007**, 3735–3737. (c) Zhao, W.; Chiuman, W.; Brook, M. A.; Li, Y. *ChemBioChem* **2007**, *8*, 727–731.

(13) Willner, I.; Shlyahovsky, B.; Zayats, M.; Willner, B. *Chem. Soc. Rev.* **2008**, *37*, 1153–1165.

(14) (a) Niazov, T.; Pavlov, V.; Xiao, Y.; Gill, R.; Willner, I. *Nano Lett.* **2004**, *4*, 1683–1687. (b) Shlyahovsky, B.; Li, D.; Katz, E.; Willner, I. *Biosens. Bioelectron.* **2007**, *22*, 2570–2576. (c) Travascio, P. *Chem. Biol.* **1998**, *5*, 505–517.

(15) (a) Li, D.; Shlyahovsky, B.; Elbaz, J.; Willner, I. *J. Am. Chem. Soc.* **2007**, *129*, 5804–5805. (b) Elbaz, J.; Moshe, M.; Shlyahovsky, B.; Willner, I. *Chem.—Eur. J.* **2009**, *15*, 3411–3418.

(16) (a) Tyagi, S.; Kramer, F. R. *Nat. Biotechnol.* **1996**, *14*, 303–308. (b) Tyagi, S.; Bratu, D. P.; Kramer, F. R. *Nat. Biotechnol.* **1998**, *16*, 49–53.

(17) Manganelli, R.; Tyagi, S.; Smith, I. Real Time PCR Using Molecular Beacons. In *Mycobacterium tuberculosis Protocols*; Parish, T., Stoker, N. G., Eds.; Humana Press: Totowa, NJ, 2001; Vol. 54, pp 295–310.

10.1021/ac901773b CCC: $40.75
Published on Web 09/25/2009

Table 1. Sequences of the Used Oligonucleotides (in 5′ to 3′ Direction)[a]

no.	sequence
(**1**)	GGGTAGGGCGGGTTGGGAACCTT**CCTGGGGGAGTATTGCGGAGGAAGGTT**CCC
(**2**)	GGGTTGGGCGGGATGGGCTAAGTAA**ATCTACGAATTCATCAGGGCTAAAGAGTGCAGAGTTACTTAG**CCC
(**3**)	Cy3−TTTCCCAACCTT**CCTGGGGGAGTATTGCGGAGGAAGGTT**CCCTTT−BHQ2
(**4**)	Cy3−TTTCCCGCTAAGTAA**ATCTACGAATTCATCAGGGCTAAAGAGTGCAGAGTTACTTAG**CCCTTT−BHQ2

[a] Aptamer sequences (bold), DNAzyme sequence (underlined), Cy3 fluorophore, BHQ2 (black hole quencher type 2).

that included the caged horseradish peroxidase-mimicking DNA in the stem region were used for the amplified detection of DNA.[19] The hybridization of the analyte DNA with the loop domains of these hairpins results in the uncaging of the DNAzyme from the stem region, which provides the catalytic readout signal for the sensing process. Here, we report on the development of "aptamer−DNAzyme hairpins" for the colorimetric detection of low-molecular-weight substrates (adenosine monophosphate) or proteins (lysozyme). We demonstrate that the aptamer−DNAzyme hairpin structures have clear advantages over analogous fluorophore−quencher beacon systems.

EXPERIMENTAL SECTION

The aptamer beacon constructs were designed using known sequences for the peroxidase-mimicking DNAzyme and the aptamers. The correct folding and thermodynamic parameters ($\Delta G°$ and melting temperature) were evaluated using the Oligo-Analyzer program (at http://www.idtdna.eu/) and cross-checked by the RNAfold[20] program (at http://rna.tbi.univie.ac.at/). The aptamer−DNAzyme constructs were purchased from Sigma Life Science (U.K.). The fluorophore−quencher-labeled beacons were obtained from Integrated DNA Technologies (U.S.A.). All oligos were HPLC-purified and freeze-dried by the respective company. Table 1 shows the sequences of the used oligonucleotides. The beacons were used as provided and diluted in 10 mM PBS to give stock solutions of 100 μM.

DNAzyme Assay. Experiments were performed in 10 mM HEPES buffer with 10 mM NaCl pH 7.1 (for the AMP (adenosine monophosphate) aptamer) or 10 mM HEPES buffer with 100 mM NaCl and 20 mM KCl pH 7.1 (for the lysozyme aptamer). The DNA constructs were used in a concentration of 1 μM. DNA was diluted in the respective buffer, heated to 90 °C for 5 min, and slowly cooled down to room temperature. Ligand was added and allowed to interact with the DNA for 30 min. For the cuvette assay, hemin and 2,2′-azino-bis(3-ethylbenzothiazoline-6-sulfonic acid) (ABTS) were added to a final concentration of 0.375 μM and 2 mM, respectively. The peroxidase-mimicking reaction was started by addition of hydrogen peroxide (final concentration of 2 mM). The color development was followed at 414 nm with a Shimadzu UV-2401 PC spectrophotometer.

Switching of AMP−Aptamer Construct. This experiment was performed in a batch of 1 mL containing 1 μM AMP−aptamer−DNAzyme construct in 10 mM HEPES buffer with 10 mM NaCl pH 7.1. After each step, a 100 μL aliquot was taken and assayed as described above. After the first sample was measured, AMP was added to yield a final concentration of 2.5 mM, and the resulting solution was incubated for 30 min and sampled for the photometric assay. Adenosine deaminase (ADA, type X from calf spleen, Sigma-Aldrich) was used as obtained. Three U (50 nkat) of ADA were added to the batch and incubated for 20 min. After taking a sample, the whole batch was heated to 80 °C for 10 min to deactivate the ADA. Thereafter, AMP was added, and the cycle was repeated as before.

Fluorescence Experiments. Experiments were performed in 10 mM HEPES buffer with 10 mM NaCl pH 7.1 (for the AMP aptamer) or 10 mM HEPES buffer with 50 mM NaCl pH 7.1 (for the lysozyme aptamer). The DNA constructs and their respective ligands were prepared as described above for the photometric assay. The fluorescence measurements were performed using a Cary Eclipse fluorimeter (Varian Inc.) after an incubation of 30 min. The Cy3 dye was excited at a wavelength of 540 nm. Fluorescence emission spectra were recorded from 554 to 610 nm.

RESULTS AND DISCUSSION

Figure 1A shows the hairpin-DNAzyme hybrid structure (**1**) for analyzing adenosine monophosphate (AMP). It consists of the AMP aptamer sequence (orange) and the horseradish peroxidase (HRP)-mimicking DNAzyme sequence (blue). The aptamer and DNAzyme sequences are bridged at the 5′- and 3′-end, respectively, by an additional sequence (gray). Similarly, a short nucleic acid tether (gray) is added to the 3′-end of the aptamer. This composition ensures that parts of the aptamer and DNAzyme sequences are caged in the duplex structure of the stem. As a result, the DNAzyme sequence cannot fold in the presence of hemin into the catalytically active G-quadruplex/hemin HRP-mimicking DNAyzme structure. In the presence of AMP, the AMP−aptamer complex is stabilized, resulting in the opening of the hairpin structure. This releases the caged HRP-mimicking DNAzyme sequence that assembles, in the presence of hemin, into the HRP-mimicking DNAzyme. Thus, the DNAzyme can catalyze the oxidation of 2 mM $ABTS^{2-}$ by H_2O_2 to $ABTS^{\bullet -}$ (λ_{max} = 414 nm; ε = 36 000 $M^{-1}\cdot cm^{-2}$), which enables the amplified colorimetric readout of the formation of the aptamer−AMP complex. To ensure the opening of the hairpin by AMP, the hairpin structure was designed by adjusting the relative stability of the stem duplex, $\Delta G°$ = −9.62 kcal·mole^{-1} to that of the aptamer−AMP complex[21] ($K_{eq} = 1.67 \times 10^5$ M^{-1}, $\Delta G°$ = 7.1 kcal·mole^{-1}). The free energy needed for unfolding is a little higher than the free energy provided by the ligand binding,

(18) (a) Li, J. J.; Tan, W. *Anal. Biochem.* **2003**, *312*, 251–254. (b) Tang, Z.; Wang, K.; Tan, W.; Li, J.; Liu, L.; Guo, Q.; Meng, X.; Ma, C.; Huang, S. *Nucleic Acids Res.* **2003**, *31*, e148.

(19) Xiao, Y.; Pavlov, V.; Niazov, T.; Dishon, A.; Kotler, M.; Willner, I. *J. Am. Chem. Soc.* **2004**, *126*, 7430–7431.

(20) Gruber, A. R.; Lorenz, R.; Bernhart, S. H.; Neubock, R.; Hofacker, I. L. *Nucleic Acids Res.* **2008**, W70–W74.

(21) Huizenga, D. E.; Szostak, J. W. *Biochemistry* **1995**, *34*, 656–665.

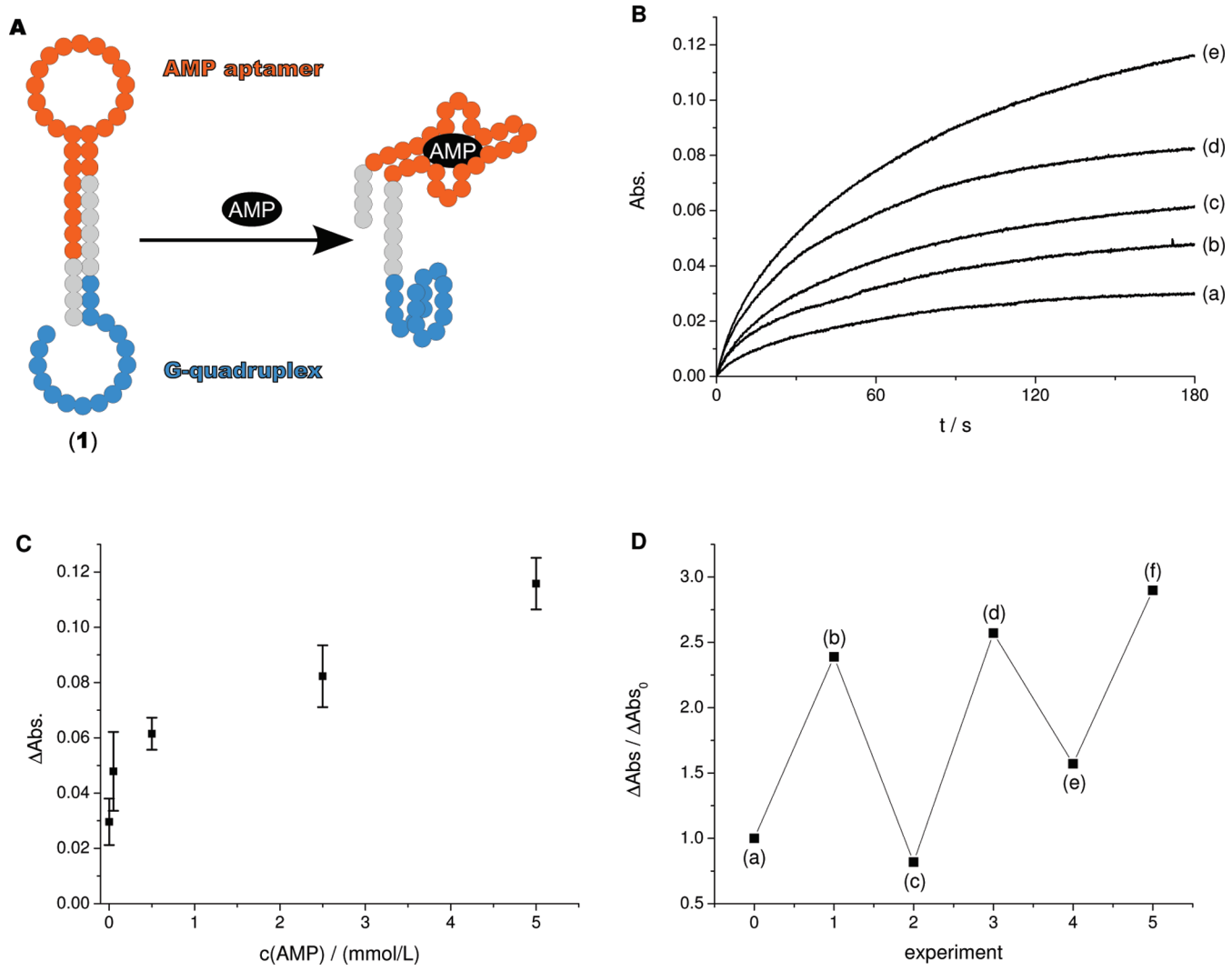

Figure 1. (A) Schematic analysis of adenosine monophosphate (AMP) by the aptamer–DNAzyme hairpin structure. (B) Time-dependent absorbance changes upon analyzing AMP by the aptamer–DNAzyme hairpin structure (**1**): (a) 0 M, (b) 50 μM, (c) 500 μM, (d) 2.5 mM, and (e) 5 mM. (C) Calibration curve corresponding to the analysis of different concentrations of AMP by the aptamer–DNAzyme hairpin structure. Absorbance changes were recorded after a fixed time-interval corresponding to 3 min. (D) The switchable sensing of AMP by the aptamer–DNAzyme system: The initially closed hairpin (a) is activated after addition of AMP (b). The separation of the aptamer–AMP complex, (c) and (e), was achieved by its reaction with adenosine deaminase. The reactivation of the sensing hairpin system was accomplished by the thermal denaturation of adenosine deaminase and addition of AMP, (d) and (f).

because also the folding of the DNAzyme contributes to the opening of the hairpin.

Figure 1B shows the time-dependent absorbance changes upon analyzing different concentrations of AMP by the hairpin structure. As higher concentrations of AMP are added, the absorbance values increase. This is consistent with the fact that the more the hairpin is opened, the higher the amounts of $ABTS^{\bullet -}$ get. One may realize that small time-dependent absorbance changes are observed even in the absence of AMP (see Figure 1B, curve (a)). This oxidation absorbance changes are due to the inefficient hemin-catalyzed oxidation of $ABTS^{2-}$ by H_2O_2 and are observed only with hemin or hemin with foreign nucleic acids. Thus, the absorbance changes depicted in Figure 1B, curve (a), may be considered as the background signal of the system under conditions where the hairpin is closed. The calibration curve for analyzing AMP is shown in Figure 1C, indicating that AMP is analyzed with a detection limit that corresponds to 50 μM.

Moreover, we switched "ON" and "OFF" the opening and closure of the hairpin structure and demonstrated the reusability of hairpin sensors. Adenosine deaminase (ADA) catalyzes the deamination of AMP to inosine monophosphate (IMP), which lacks the high affinity for the aptamer sequence. Indeed, the ADA-stimulated deamination of AMP to IMP was recently used to separate the AMP–aptamer complex and to activate DNA machines such as a walker[22] or tweezers.[23] Accordingly, the hairpin (**1**) was used to analyze AMP as a first sensing cycle, Figure 1D, point (b). Subsequently, the system was interacted with ADA. The absorbance of the system leveled-off to a constant value, implying that the AMP–aptamer complex was separated, resulting in the refolding of the hairpin structure, a process that is accompanied by the separation of the HRP–DNAzyme structure and the

(22) Elbaz, J.; Tel-Vered, R.; Freeman, R.; Yildiz, H.; Willner, I. *Angew. Chem., Int. Ed.* **2009**, *48*, 133–137.
(23) Elbaz, J.; Moshe, M.; Willner, I. *Angew. Chem., Int. Ed.* **2009**, *48*, 3834–3837.

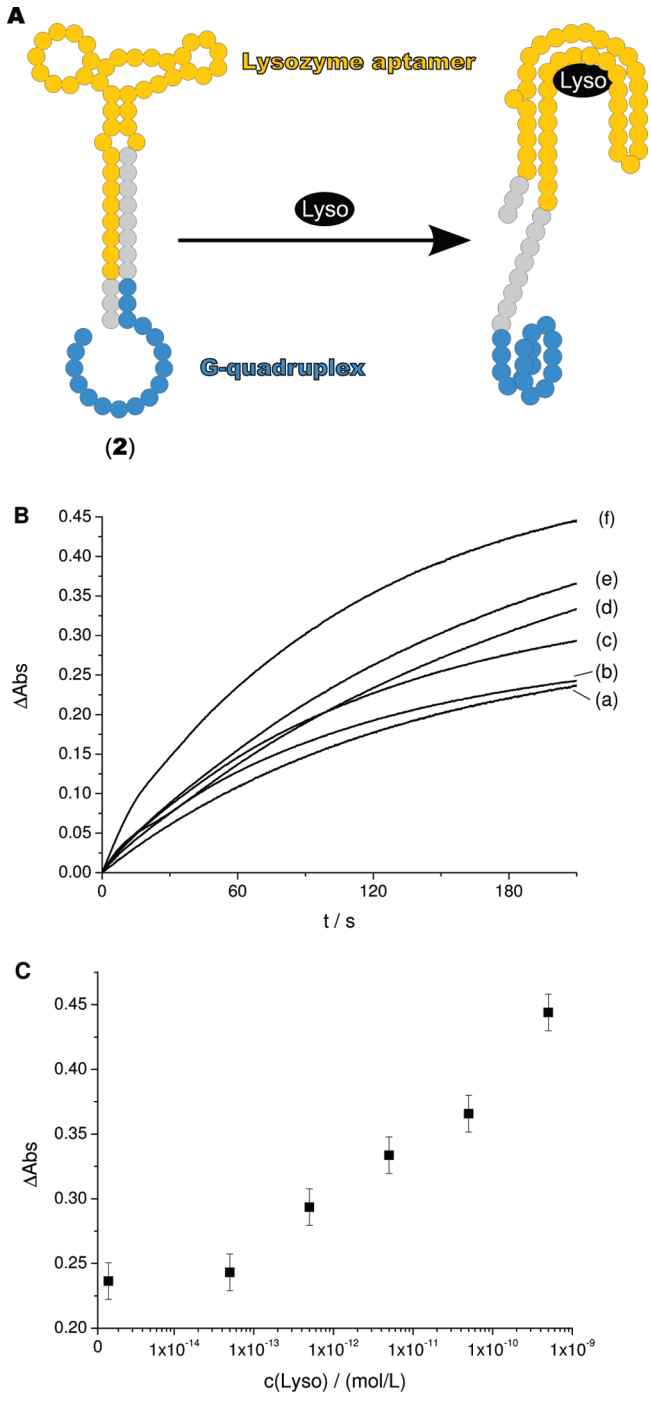

Figure 2. (A) Schematic analysis of lysozyme by the aptamer–DNAzyme hairpin structure. (B) Time-dependent absorbance changes upon analyzing lysozyme by the aptamer–DNAzyme hairpin structure (**2**): (a) 0 pM, (b) 0.05 pM, (c) 0.5 pM, (d) 5 pM, (e) 50 pM, and (f) 500 pM. (C) Calibration curve corresponding to the analysis of different concentrations of lysozyme by the aptamer–DNAzyme hairpin structure. Absorbance changes were recorded after a fixed time-interval corresponding to 3.5 min.

protection of its sequence in the hairpin stem region (Figure 1D, point (c)). Subsequently, the system was heated to 80 °C for 10 min to denaturate ADA, and the resulting assembly was used to analyze AMP in a second cycle, Figure 1D, point (d). The hairpin structure is reopened, and the release of the HRP-mimicking DNAzyme allows the colorimetric readout of the analysis of AMP. By the cyclic treatment of the system with ADA and thermal

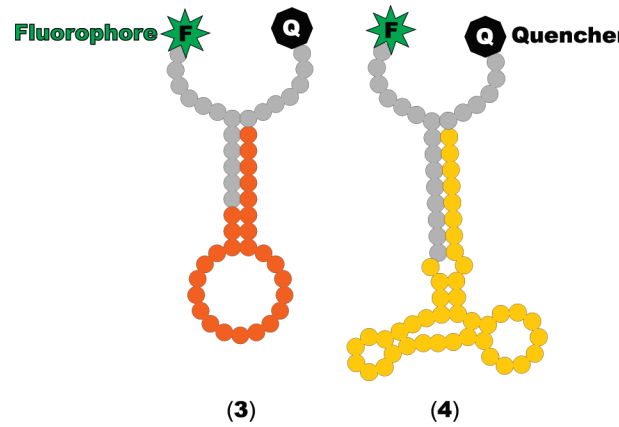

Figure 3. The fluorophore–quencher-modified aptamer hairpins for the fluorescence analysis of adenosine monophosphate (**3**) and lysozyme (**4**).

denaturation of the enzyme, the hairpin structure (**1**) was regenerated for further analysis cycles of AMP. One may realize that upon the regeneration of the hairpin structure (**1**) with ADA, a slight increase in the color of the system is obtained upon addition of the same concentration of AMP. Similarly, the absorbance value of the "inactive" closed hairpin structure is higher, as the number of regeneration cycles increases. This is attributed to the fact that the ADA-generated IMP exhibits some affinity to the AMP aptamer and functions as a competitive binder to the aptamer site.[24] Furthermore, IMP was reported as an inhibitor of ADA.[25] Thus, upon increasing the number of cycles, the inhibition of ADA is more effective due to the accumulation of IMP. It should be noted, however, that the slight competitive activation of (**1**) by IMP does not affect the performance of the system toward the analysis of AMP, since the sensing of AMP examines the absorbance difference (ΔAbs) between the AMP activated and mute systems, where [AMP] = 0 M.

In analogy, we have designed the aptamer hairpin structure (**2**) for the detection of lysozyme (Lyso). The system consists of the aptamer sequence (yellow) that exhibits partial complementarity in the loop region. The aptamer is tethered at its 3′-end to a short CCC sequence (gray) and at its 5′-end to a longer tether (gray) that is complementary to a domain of the aptamer that leads to the formation of the stem part of the hairpin (Figure 2A). The added nucleic acid tether (gray) bridges also the aptamer sequence to the HRP-mimicking DNAyzme sequence (blue). Thus, a part of the DNAzyme sequence yields a stable duplex domain in the stem region, which cages the DNAzyme into a protected, catalytically inactive configuration. The addition of lysozyme results in the formation of the lysozyme–aptamer complex, a process that separates the duplex structure of the stem. The deprotection of the DNAyzme sequence into a single-stranded chain allows its self-assembly to the catalytically active hemin-G-quadruplex HRP-mimicking DNAzyme structure in the presence of hemin. The biocatalyzed oxidation of $ABTS^{2-}$ by H_2O_2 to the colored product $ABTS^{\bullet-}$ provides an optical signal for the formation of the lysozyme–aptamer complex. It should be noted that the aptamer hairpin construct was designed in

(24) Elowe, N. H.; Nutiu, R.; Allali-Hassani, A.; Cechetto, J. D.; Hughes, D. W.; Li, Y.; Brown, E. D. *Angew. Chem., Int. Ed.* **2006**, *45*, 5648–5652.
(25) Fox, I. H.; Kelley, W. N. *Annu. Rev. Biochem.* **1978**, *47*, 655–686.

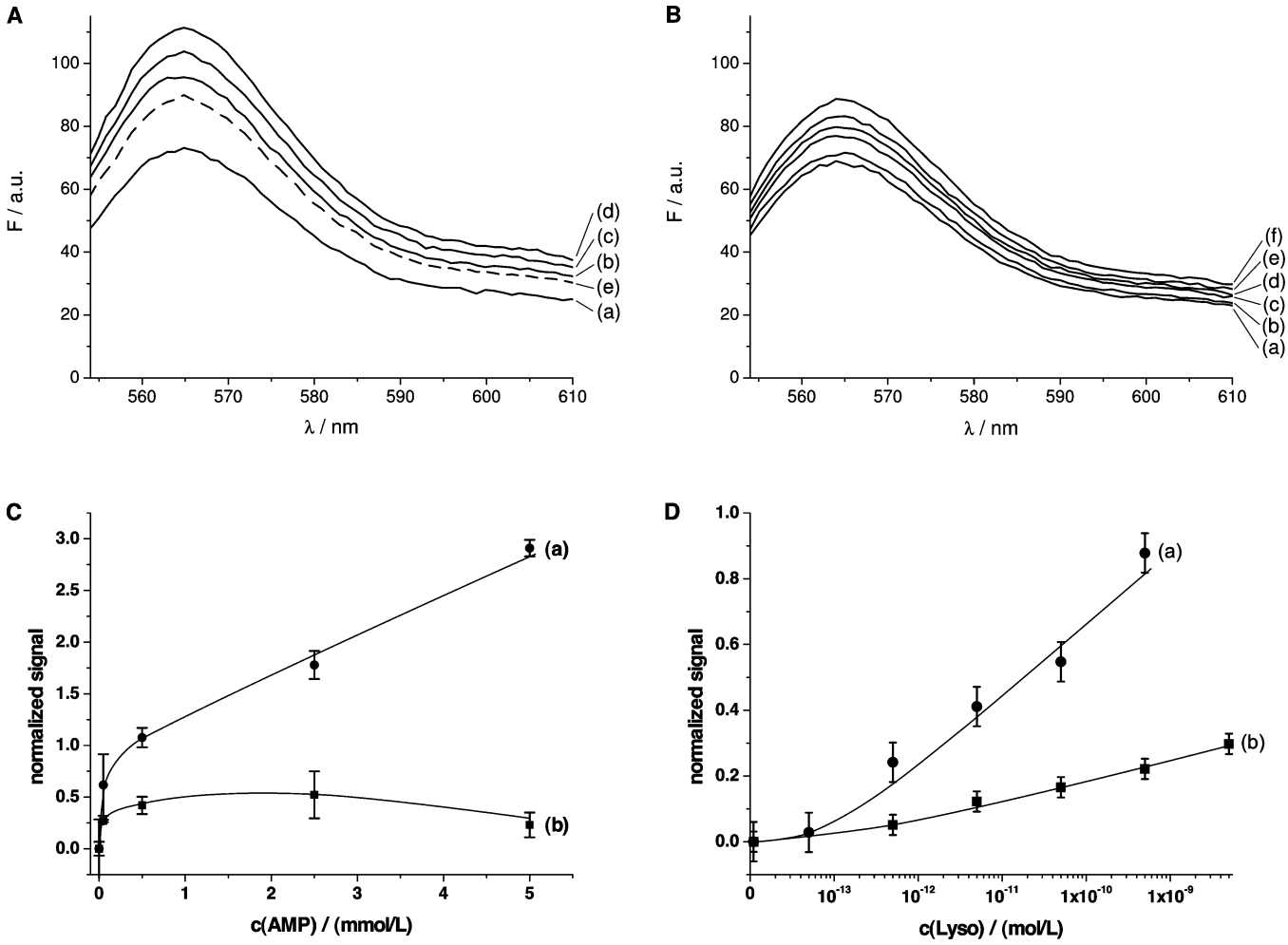

Figure 4. (A) Fluorescence spectra corresponding to the analysis of variable concentrations of AMP by the fluorophore−quencher hairpin structure (**3**): (a) 0 mM, (b) 0.1 mM, (c) 0.5 mM, (d) 2.5 mM, and (e) 5 mM (dashed line). Fluorescence spectra were recorded after a fixed time-interval of 30 min, allowing the opening of (**3**) by AMP. (B) Fluorescence spectra corresponding to the analysis of variable concentrations of lysozyme by the fluorophore−quencher hairpin structure (**4**): (a) 0 pM, (b) 0.5 pM, (c) 5 pM, (d) 50 pM, (e) 500 pM, and (f) 5 nM. Fluorescence spectra were recorded after a fixed time-interval of 30 min, allowing the opening of (**4**) by lysozyme. (C) Comparison of the calibration curves corresponding to the analysis of AMP by the: (a) aptamer−DNAzyme hairpin structure (**1**) and (b) fluorophore−quencher hairpin (**3**). (D) Comparison of the calibration curves corresponding to the analysis of lysozyme by the: (a) aptamer−DNAzyme hairpin structure (**2**) and (b) the fluorophore−quencher hairpin (**4**).

such a way that, in the absence of lysozyme, the duplex stem formation and protection of the DNAzyme are favored ($\Delta G^\circ = -10.97$ kcal·mole^{-1}), but in the presence of lysozyme, the formation of the lysozyme−aptamer complex is energetically favored ($\Delta G^\circ = -10.2$ kcal·mole^{-1}).[26]

Figure 2B shows the time-dependent absorbance changes observed upon analyzing different concentrations of lysozyme using the hairpin structure (**2**). As the concentration of lysozyme increases, the absorbance changes are enhanced, consistent with the higher contents of the open hairpin structure that leads to the biocatalyzed oxidation of $ABTS^{2-}$. The resulting calibration curve, Figure 2C, indicates that the hairpin (**2**) enabled the analysis of lysozyme with a detection limit corresponding to 0.5 pM.

To evaluate the sensing performance of the aptamer−DNAzyme hairpin structures (**1**) and (**2**), we compared the analysis of AMP and lysozyme by these catalytic hairpins to the optical detection of the same analytes by the classical fluorophore−quencher aptamer−hairpin structures (**3**) and (**4**) (see Figure 3). In the beacon (**3**), the aptamer sequence (orange) is present in the single-stranded loop as well as the stem structure. The fluorophore and quencher are linked to single-stranded nucleic acid tethers (gray) linked to the stem. It should be noted that the single-stranded tethers are essential to yield the fluorophore−quencher separation upon the opening of the direct attachment of the fluorophore−quencher pair to the stem ends, which did not lead to any noticeable fluorescence changes upon the reaction of (**3**) with AMP. Figure 4A shows the fluorescence changes of (**3**) upon interaction with variable concentrations of AMP. As expected, the fluorescence intensity is elevated as the concentration of AMP increases, consistent with the opening of the hairpin structure. Interestingly, the fluorescence intensity declines with high AMP concentrations, i.e., [AMP] = 5 mM. This quenching effect was also observed in a control experiment in which the hairpin beacon (**4**), containing the lysozyme-binding aptamer, was subjected to an equally high AMP concentration (see Figure S1 in the Supporting Information). Thus, the analysis of AMP by the fluorescence method becomes less accurate as

the concentration of AMP increases, due to the quenching of the fluorophore by AMP.

Similar considerations, as described above for the hairpin (**3**), were also taken into account when we designed the beacon (**4**) for the analysis of lysozyme. Figure 4B shows the fluorescence intensities of the system upon the interaction of (**4**) with variable concentrations of lysozyme. As before, the fluorescence intensities of the systems are higher as the concentration of lysozyme increases. For example, a 29.8% increase in the fluorescence intensity of this system is observed at a lysozyme concentration corresponding to 5 nM.

The analysis of AMP or lysozyme by the hairpin-DNAzyme conjugates and the respective beacons utilize, however, two different transduction signals (absorbance and fluorescence, respectively). Accordingly, to compare the analysis of the two targets by the hairpin-DNAzyme and beacon structures, we normalized the readout signals of the structures ($\Delta Abs/\Delta Abs_0 - 1$ vs $\Delta F/\Delta F_0 - 1$), Figure 4C,D. We may realize that the readout signal for analyzing [AMP] $= 2.5 \times 10^{-5}$ M by the aptamer−DNAzyme hairpin is ca. 3.4-fold higher than the readout signal observed with the respective beacon. Similarly, the readout signal for analyzing lysozyme (at [Lyso] $= 5 \times 10^{-10}$ M) by the aptamer−DNAzyme hairpin is ca. 3-fold higher than the signal generated by the fluorophore−quencher beacon.

CONCLUSIONS

In conclusion, we extended the paradigm of sensing by nucleic acid hairpin structures to the analysis of low-molecular-weight substrates (AMP) or proteins (lysozyme) by aptamer-based hairpin structures. Specifically, we find that predesigned aptamer−DNAzyme hairpins are useful constructs for the detection of the respective aptamer−substrate complexes. We also reveal that aptamer-based beacon structures are inefficiently separated by the analytes. This is presumably due to the relative weak binding interactions of the aptamer−substrate complexes, as compared to the energetics of the stem. The successful analysis of the target by the aptamer−DNAzyme hybrids may be attributed to the amplifying effect of the released DNAzyme. That is, even the partial opening of the hairpin structure is translated to a high readout signal generated by the DNAzyme.

(26) Cox, J. C.; Ellington, A. D. *Bioorg. Med. Chem.* **2001**, *9*, 2525–2531.

ACKNOWLEDGMENT

This study was supported by the Israel Science Foundation. C.T. acknowledges a Minerva fellowship. The authors thank Johann Elbaz for helpful suggestions and assistance in designing the hairpins. C.T. and S.S. contributed equally to this work.

SUPPORTING INFORMATION AVAILABLE

Additional information on the observed quenching by AMP is provided. This material is available free of charge via the Internet at http://pubs.acs.org.

Received for review August 6, 2009. Accepted August 31, 2009.

AC901773B